Simple Null-Steering OFDM Adaptive Array Antenna for Doppler-Shifted Signal Suppression

Shinsuke Hara, *Member, IEEE*, Shuichi Hane, and Yoshitaka Hara, *Member, IEEE*

***Abstract*—A new null-steering method to suppress Doppler-shifted signals is proposed for orthogonal frequency-division multiplexing adaptive array antenna. The proposed array antenna has a simple structure and can steer nulls for interfering signals even with small Doppler shifts by forcing virtual subcarrier outputs to be zero. A multistep recursive least-square algorithm is proposed to control the array weights and the bit-error rate and antenna pattern are evaluated by computer simulation.**

***Index Terms*—Adaptive array antenna, Doppler shift, null steering, orthogonal frequency-division multiplexing (OFDM).**

I. Introduction

ORTHOGONAL frequency-division multiplexing (OFDM) has a high spectral utilization efficiency by allowing the power spectra of adjacent subcarriers to overlap so as to minimize the required signal bandwidth. Furthermore, OFDM is insensitive to multipath fading encountered in wireless channels, because a guard interval (or a cyclic prefix) is inserted in each OFDM symbol so as to eliminate intersymbol and intersubcarrier interference caused by the multipath propagation. These two excellent characteristics have made OFDM attractive and advantageous in high-speed and high-reliable data transmission in wireless channels and have been adopted as standards in terrestrial digital broadcasting [1], [2] and high-data-rate wireless local area networks (LANs) [3]–[6].

In conjunction with terrestrial digital broadcasting, OFDM is also adopted as a standard for a portable digital transmission system to support television program contribution [7], which is called the field pickup unit (FPU). In the FPU, there are seven frequency bands allocated from 5.85 to 13.25 GHz and the system is specified to cope with the velocity of portable terminal up to 240 km/h (150 mi/h). For the case of the velocity of the terminal $= 240$ km/h, which is typical in the data transmission between a base station and a helicopter, and the subcarrier separation $= 10.0$ kHz, the Doppler shift reaches approximately 30.0% in terms of subcarrier separation. This means that the system should be designed so as to cope with such a large Doppler shift.

Consider the data transmission from a cruising mobile to a stationary base station. In the OFDM standards in broadcasting applications, OFDM symbols are transmitted in a continuous mode with continuous or scattered pilots embedded in the transmitted signal [1], [2], [7]. Therefore, as long as the received signal has a single Doppler shift, the receiver can successfully receive the desired signal even if it is composed of several multipath components and the value of the Doppler shift is so large. However, when the receiver suddenly receives multipath components with different large Doppler shifts because of the difference in their directions of arrivals (DoAs), they drastically degrade the bit-error rate (BER) performance.

For suppression of large Doppler-shifted signals, use of an adaptive array antenna could be effective [8]. There are two types in OFDM adaptive array antennas, such as a post-fast Fourier transform (post-FFT) type [9] and a pre-FFT type [10]–[12]. The post-FFT array antenna equips one FFT processor with each array branch. The attainable BER performance is better, but it requires a high computational complexity because the number of array weights to be controlled is given by the number of array elements times the number of subcarriers. For OFDM schemes with hundreds of subcarriers, it would be unrealizable. On the other hand, the pre-FFT array antenna requires only one FFT processor and it can reduce the computational complexity by tolerating a slight performance degradation.

The adaptive array antenna is workable as a beamformer and a null steerer. The beamforming adaptive array antenna needs to estimate at least the DoA or the channel-impulse response for the desired components in the received signal and the estimation requires observation of the received signal [8]. When the differences of Doppler shifts among the received components are so small, they receiver cannot distinguish between the desired ones and the interfering Doppler-shifted ones in a short observation period. For instance, observation of several tens of OFDM symbols is required to identify a Doppler-shifted signal with 1% subcarrier separation, although it gives an intolerable degradation to the BER performance. On the other hand, the null-steering adaptive array antenna does not try to effectively catch only the desired components, but, as shown in this paper, it can steer nulls for the Doppler-shifted components by forcing virtual subcarrier outputs to be zero [11], [12]. So far, virtual

Manuscript received December 10, 2002; revised November 14, 2003, March 12, 2004, and July 15, 2004. This work was supported in part by the research and development support scheme for funding selected IT proposals 2002, top priority research and development to be focused (frequency resources development) of the Ministry of Public Management, Home Affairs, Posts and Telecommunications of Japan. The review of this paper was coordinated by Dr. K. Molnar.

S. Hara is with the Department of Electronic, Information System, and Energy Engineering, Graduate School of Engineering, Osaka University, Osaka 565-0871, Japan (e-mail: hara@comm.eng.osaka-u.ac.jp).

S. Hane is with Tokyo Electric Power Company, Inc., Tokyo 100-8560, Japan.

Y. Hara is with the Mitsubishi Electric Information Technology Centre Europe B.V. (ITE), Rennes 35708, France.

Digital Object Identifier 10.1109/TVT.2004.838834

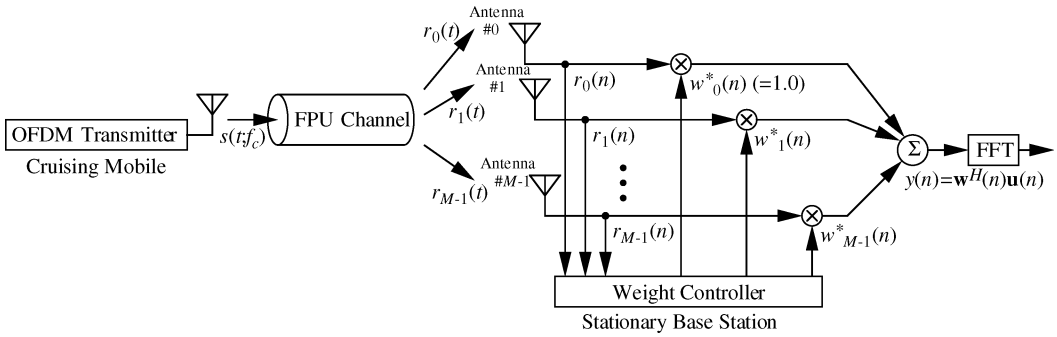

Fig. 1. System model.

subcarriers have been exploited in the estimation and synchronization problems of an OFDM system: a carrier offset estimator, a blind channel-estimation method, and a time-carrier offset estimator are proposed by [13], [14], and [15], respectively. However, to the authors' best knowledge, no paper has exploited virtual subcarriers for weight control in the adaptive array antenna.

This paper proposes a null-steering method to suppress Doppler-shifted signals for a pre-FFT-type OFDM adaptive array antenna. The method is simple and requires no special signal to control the array weights.

This paper is organized as follows. Section II shows the system model and Section III presents the principle of the proposed null-steering method. Section IV shows the computer simulation results and discusses the performance of the proposed null-steering method. Finally, Section V presents the conclusion.

II. System Model

Fig. 1 shows the system model in which a train of OFDM signals is transmitted from a cruising mobile, through an FPU channel, to a stationary base station. The base station has an adaptive array antenna with M antenna elements. Here, to deal with the OFDM null-steering as a narrow-band signal processing, the following assumption is made [8], [16]:

$$\frac{D_{\text{array}}}{\lambda} \ll \frac{f_c}{B_{\text{OFDM}}} \tag{1}$$

where D_{array} and B_{OFDM} are the maximum dimension of the array antenna and the bandwidth of the OFDM signal, respectively, and f_c and λ are the frequency and wavelength of the carrier, respectively.

The transmitted OFDM signal is given by

$$s(t;f_c) = \sum_{i=-\infty}^{+\infty} \sum_{k=0}^{K_{sc}-1} c_{ki} e^{j2\pi f_k(t-iT_s)} g(t-iT_s) \tag{2}$$

$$g(t) = \begin{cases} 1, & 0 < t \le T_s \\ 0, & \text{otherwise} \end{cases} \tag{3}$$

$$f_k = f_c + k\Delta f_{sc} \tag{4}$$

$$\Delta f_{sc} = \frac{1}{t_s} \tag{5}$$

$$T_s = \Delta_G + t_s \tag{6}$$

where K_{sc} is the number of subcarriers; c_{ki}, f_k, and $g(t)$ are the ith information symbol transmitted over the kth subcarrier, the frequency of the kth subcarrier and the rectangular pulse waveform, respectively; Δ_G, t_s, and T_s are the guard interval length, the useful symbol length, and the OFDM symbol length, respectively; and Δf_{sc} is the subcarrier separation. Fig. 2 shows a subcarrier arrangement in the equivalent baseband expression. In this figure, there are two kinds of subcarriers: "data" and "virtual." The data subcarriers including "pilot" subcarriers convey information, whereas the virtual subcarriers convey zero information; in other words, they are not used for actual data transmission. In Fig. 2, the subcarriers with numbers 0-K_{low}, K_{mid} and K_{high}-to-$(K_{sc}-1)$ are the virtual subcarriers and the remaining subcarriers are the data subcarriers. Here, f_{v0}, f_{v1}, and f_{v2} mean the frequencies of the K_{low}th, K_{mid}th, and K_{high}th virtual subcarriers, respectively.

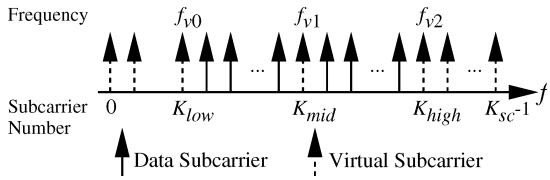

Fig. 2. Subcarrier arrangement.

Through the FPU channel, the transmitted OFDM signal is subject to multipath fading and Doppler shifts. When the OFDM signal experiences a signal Doppler shift, the hth multipath component of OFDM signal received at the mth antenna element is given by

$$r_{Dh,m}(t;f_c+\Delta f_D) = \alpha_{Dh,m} s(t-\tau_{Dh};f_c+\Delta f_D) \quad (h=0,\ldots,L_D-1) \tag{7}$$

where Δf_D is the value of Doppler shift, $\alpha_{Dh,m}$ is the complex-valued channel loss for the hth multipath component at the mth antenna element, τ_{Dh} is the real-valued time delay for the hth multipath component, and L_D is the number of multipath components. Here, without loss of generality, the multipath components are numbered so as to make $\tau_{Dh} < \tau_{D(h+1)}$ $(h=0,\ldots,L_D-2)$ and τ_{D0} is set to 0.

As long as the received signal is composed of a single Doppler-shifted component, the base station can accurately estimate the value of the Doppler shift with the aid of the pilot signals

$$f_l = f_c + \Delta f_D \tag{8}$$

where f_l is the frequency of the local oscillator at the base station. The hth mutipath component after downconversion with f_l is written as

$$r_{Dh,m}(t)=r_{Dh,m}(t;f_c+\Delta f_D-f_l)=\alpha_{Dh,m}s(t-\tau_{Dh};f_c=0). \tag{9}$$

In the following, $r_{Dh,m}(t;f_c+\Delta f_D)$ $(h=0,\ldots,L_D-1)$ is dealt with as a desired component, so it means that the desired OFDM signal is composed of L_D multipath components with the same Doppler shift of Δf_D.

On the other hand, when some OFDM signals with the other values of Doppler shifts suddenly interfere with the desired OFDM signal, the lth component of the interfering signal received at the mth antenna element is written as

$$r_{Il,m}(t;f_c+\Delta f_{Il})=\alpha_{Il,m}s(t-\tau_{Il};f_c+\Delta f_{Il}), \quad l=0,\ldots,L_I-1 \tag{10}$$

where Δf_{Il} and τ_{Il} $(\tau_{Il}<\tau_{I(l+1)})$ are the Doppler shift and time delay of the lth interfering component, respectively; $\alpha_{Il,m}$ is the channel loss for the lth interfering component at the mth antenna element; and L_I is the number of interfering signals. The local oscillator is synchronized only to the received desired signal and is insensitive to the sudden arrivals of the interfering signals. Therefore, the lth interfering component after downconversion with f_l is written as

$$r_{Il}(t)=\alpha_{Il}s(t-\tau_{Il};f_c=\Delta f'_{Il}) \tag{11}$$

$$\Delta f'_{Il}=\Delta f_{Il}-\Delta f_D. \tag{12}$$

In the following, $\Delta f'_{Il}$ is just called "the Doppler shift" for the lth interfering component.

Consequently, the received signal at the mth antenna element in the equivalent baseband expression is composed of the desired components, the interfering components, and an additive white Gaussian noise (AWGN)

$$r_m(t)=\sum_{h=0}^{L_D-1}r_{Dh,m}(t)+\sum_{l=0}^{L_I-1}r_{Il,m}(t)+\nu_m,(t), \quad m=0,\ldots,M-1 \tag{13}$$

where $\nu_m(t)$ is the complex-valued AWGN with the power of σ_n^2 at the mth antenna element. Here, it is assumed that the noise is mutually independent at each antenna element.

III. Principle of the Null-Steering Method

A. Use of Virtual Subcarrier Outputs

The received signal is sampled to control the array weights with an adaptive digital signal-processing techniques. Assume that the guard interval is N_G samples long and the useful symbol is N_U samples long. Setting the first sampling instant in the ith OFDM symbol for the first arrival desired signal $(h=0)$ to $n=0$, the array output at a sampling instant of n is written as

$$y(n)=\mathbf{w}^H(n)\mathbf{r}(n) \tag{14}$$

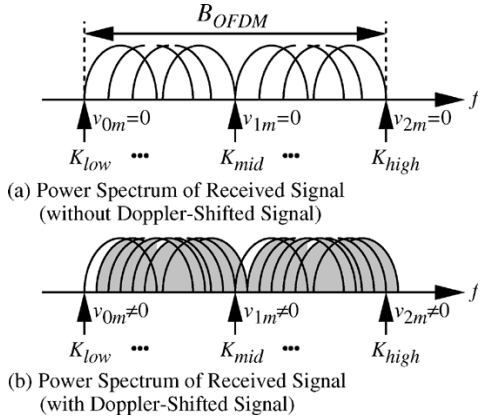

Fig. 3. Principle of null steering.

where H denotes Hermitian transpose. In (14), $\mathbf{r}(n)$ and $\mathbf{w}(n)$ are the received signal vector ($M\times 1$) and the weight vector ($M\times 1$), respectively, which are given by

$$\mathbf{r}(n)=[r_0(n),\ldots,r_m(n),\ldots,r_{M-1}(n)]^T \tag{15}$$

$$\mathbf{w}(n)=[w_0(n),\ldots,w_m(n),\ldots,w_{M-1}(n)]^T \tag{16}$$

where T denotes transpose.

Fig. 3 shows the principle of the interference suppression. At the mth antenna element $(0\le m\le M-1)$, when the received signal contains only the desired components, the outputs at the K_{low}th, K_{mid}th, and K_{high}th virtual subcarriers are always zero. However, once it contains the Doppler-shifted interfering components as well as the desired components, they become nonzero. Therefore, if controlling the array weights so as to force the virtual subcarrier outputs to be zero, the array antenna can steer nulls toward the interfering components.

B. Calculation of Virtual Subcarrier Outputs

To derive the array weight control algorithm, define the jth virtual subcarrier output vector ($M\times 1$) as (j =0, 1, 2; see Fig. 2)

$$\mathbf{v}_j(n)=[v_{j0}(n),\ldots,v_{jm}(n),\ldots,v_{j(M-1)}(n)]^T \tag{17}$$

where $v_{jm}(n)$ is the jth virtual subcarrier output of the mth antenna element at the nth sampling instant. With the following complex-valued sinusoidal function, $v_{jm}(n)$ is written as

$$v_{jm}(n)=\sum_{q=0}^{N_U-1}b_j(q)r_m(n-q) \tag{18}$$

$$b_j(q)=e^{-j2\pi(f_{vj}q/N_U)}. \tag{19}$$

Note that calculation of the jth virtual subcarrier output means downconversion of the received signal with the frequency of the jth virtual subcarrier; therefore, it takes N_U samples to give the first output.

With (13), (18) can be decomposed into the following three components:

$$v_{jm}(n) = \sum_{h=0}^{L_D-1} v_{Dh,jm}(n) + \sum_{l=0}^{L_I-1} v_{Il,jm}(n) + v_{\nu,jm}(n) \tag{20}$$

$$v_{Dh,jm}(n) = \sum_{q=0}^{N_U-1} b_j(q) r_{Dh,m}(n-q) \tag{21}$$

$$v_{Il,jm}(n) = \sum_{q=0}^{N_U-1} b_j(q) r_{Il,m}(n-q) \tag{22}$$

$$v_{\nu,jm}(n) = \sum_{q=0}^{N_U-1} b_j(q) \nu_m(n-q) \tag{23}$$

where $v_{Dh,jm}(n)$ and $v_{Il,jm}(n)$ are the jth virtual subcarrier outputs of the mth antenna element at the nth sampling instant for the hth desired component and the lth interfering component, respectively, and $v_{\nu,jm}(n)$ is the noise component in the jth virtual subcarrier output.

The proposed null-steering method sets the start of the downconversion at $n = T_W$, so the number of outputs employable for the weight control is $N_G - T_W + 1$. For the interfering component, $\Delta f'_{Il} \neq 0$ results in

$$v_{Il,jm}(n) \neq 0, \qquad (N_U + T_W - 1 \leq n \leq N_U + N_G - 1 \tag{24}$$

so the array antenna annihilates all the interfering components by nulling out.

Fig. 4(a) shows the downconversion for the desired component with $\tau_{Dh} \leq T_W$. In this case, as the period of the downconversion contains no boundary between the $(i-1)$th and ith OFDM symbols, the virtual subcarrier outputs *do not* contain the desired component

$$v_{Dh,jm}(n) = 0, \qquad N_U + T_W - 1 \leq n \leq N_U + N_G - 1 \tag{25}$$

so the array antenna steers no null toward the desired component. On the other hand, Fig. 4(b) shows the downconversion for the desired component with $\tau_{Dh} > T_W$. In this case, as the period of the downconversion contains the boundary between the $(i-1)$th and ith OFDM symbols, the virtual subcarrier outputs *do* contain the desired component

$$v_{Dh,jm}(n) \neq 0, \qquad N_U + T_W - 1 \leq n < N_U + \tau_{Dh} - 1 \tag{26}$$

so the array antenna steers a null toward the desired component. In this way, the proposed array antenna steers nulls toward all the interfering components and the desired components whose time delays range in $[T_W + 1, N_G - 1]$. Therefore, a larger value of T_W reduces the number of desired components suppressed; on the other hand, it reduces the number of iterations that are employable in the control algorithm.

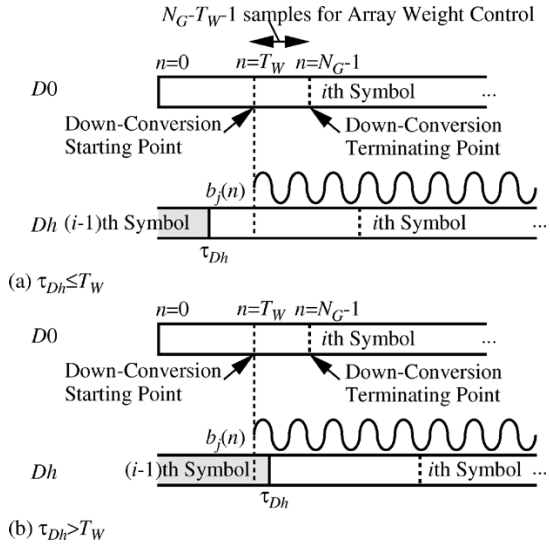

Fig. 4. Calculation of virtual subcarrier output.

C. Multistep Recursive Least-Square (RLS) Algorithm

The error between the desired response and the combined jth virtual subcarrier output is written as

$$e_j(n) = 0 - \mathbf{w}^H(n)\mathbf{v}_j(n). \tag{27}$$

The minimization problem for the RLS algorithms given by [17]

$$\text{minimize } |\varepsilon_R(n)|^2 = \sum_{j=0}^{2} \sum_{p=N_U+T_W-1}^{n} \lambda^{n-p} |e_j(p)|^2, \quad N_U + T_W - 1 \leq n \leq N_U + N_G - 1 \tag{28}$$

where λ is a forgetting factor. Equation (28) has a solution of $\mathbf{w}(n) = \mathbf{0}$, so a constraint is required to avoid the trivial solution; for instance

$$\text{subject to} \quad w_0(n) = 1. \tag{29}$$

Therefore, the cost function in (28) is rewritten as

$$|\varepsilon_R(n)|^2 = \sum_{j=0}^{2} \sum_{p=N_U+T_W-1}^{n} |0 - (w_0^*(p) v_{j0}(p) + \mathbf{w}'^H(p)\mathbf{v}'_j(p))|^2 \tag{30}$$

$$\mathbf{v}'_j(p) = [v_{j1}(p), \ldots, v_{jm}(p), \ldots, v_{j(M-1)}(p)]^T \tag{31}$$

$$\mathbf{w}'(p) = [w_1(p), \ldots, w_m(p), \ldots, w_{M-1}(p)]^T \tag{32}$$

where $\mathbf{v}'_j(p)$ and $\mathbf{w}'(p)$ are newly defined jth virtual subcarrier output vector $((M-1)\times 1)$ and weight vector $((M-1)\times 1)$, respectively.

The optimum weight vector $\widehat{\mathbf{w}'}(n)$ for the cost function of (28) is given by the solution of

$$\mathbf{\Phi}(n)\widehat{\mathbf{w}'}(n) = \mathbf{z}(n) \tag{33}$$

$$\mathbf{\Phi}(n) = \sum_{j=0}^{2} \mathbf{\Phi}_j(n) \tag{34}$$

$$\mathbf{z}(n) = \sum_{j=0}^{2} \mathbf{z}_j(n) \tag{35}$$

$$\mathbf{\Phi}_j(n) = \sum_{p=N_U-1}^{n} \lambda^{n-p} \mathbf{v}'_j(p) \mathbf{v}'^{H}_j(p) \tag{36}$$

$$\mathbf{z}_j(n) = -\sum_{p=N_U-1}^{n} \lambda^{n-p} \mathbf{v}'_j(p) v^*_{j0}(p) \tag{37}$$

where $\mathbf{\Phi}_j(n)$ and $\mathbf{z}_j(n)$ are the correlation matrix ($(M-1) \times (M-1)$) and the correlation vector ($(M-1)\times 1$) for the jth virtual subcarrier output, respectively.

The recursive equation for the correlation matrix $\mathbf{\Phi}(n)$ is given by

$$\mathbf{\Phi}(n) = \lambda \mathbf{\Phi}(n-1) + \sum_{j=0}^{2} \mathbf{v}'_j(n) \mathbf{v}'^{H}_j(n). \tag{38}$$

Similarly, the recursive equation for the correlation vector is given by

$$\mathbf{z}(n) = \lambda \mathbf{z}(n-1) - \sum_{j=0}^{2} \mathbf{v}'_j(n) v^*_{j0}(n). \tag{39}$$

RLS algorithms generally require calculation of $\mathbf{\Phi}^{-1}(n)$, but the last term in (38) is composed of the sum of the three matrices, so the matrix inversion lemma cannot be directly applied [17].

Now, divide (38) into the following three steps:

$$\mathbf{\Phi}'_0(n) = \lambda_0 \mathbf{\Phi}'_2(n-1) + \mathbf{v}'_0(n) \mathbf{v}'^{H}_0(n) \tag{40}$$

$$\mathbf{\Phi}'_1(n) = \lambda_1 \mathbf{\Phi}'_0(n) + \mathbf{v}'_1(n) \mathbf{v}'^{H}_1(n) \tag{41}$$

$$\mathbf{\Phi}'_2(n) = \lambda_2 \mathbf{\Phi}'_1(n) + \mathbf{v}'_2(n) \mathbf{v}'^{H}_2(n) \tag{42}$$

where λ_j (j =0,1,2) is a forgetting factor and the size of $\mathbf{\Phi}'_j(n)$ (j =0,1,2) is $(M-1) \times (M-1)$. Similarly, divide (39) into the following three steps:

$$\mathbf{z}'_0(n) = \lambda_0 \mathbf{z}'_2(n-1) - \mathbf{v}'_0(n) v_{00}{}^*(n) \tag{43}$$

$$\mathbf{z}'_1(n) = \lambda_1 \mathbf{z}'_0(n) - \mathbf{v}'_1(n) v_{10}{}^*(n) \tag{44}$$

$$\mathbf{z}'_2(n) = \lambda_2 \mathbf{z}'_1(n) - \mathbf{v}'_2(n) v_{20}{}^*(n) \tag{45}$$

where the size of $\mathbf{z}'_j(n)$ (j =0,1,2) is $(M-1) \times 1$.

From each pair of the recursive equations for the correlation matrix and vector, namely, (40) and (43), (41) and (44), and (42) and (45), an RLS algorithm can be derived. Finally, the following RLS algorithm can be obtained [17] as

$$\mathbf{k}_0(n) = \frac{\lambda_0{}^{-1} \mathbf{P}_2(n-1) \mathbf{v}'_0(n)}{1 + \lambda_0{}^{-1} \mathbf{v}'^{H}_0(n) \mathbf{P}_2(n-1) \mathbf{v}'_0(n)} \tag{46}$$

$$\xi_0(n) = -v_{00}(n) - \mathbf{w}'^{H}_2(n-1) \mathbf{v}'_0(n) \tag{47}$$

$$\mathbf{P}_0(n) = -\lambda_0{}^{-1} \mathbf{P}_2(n-1) - \lambda_0{}^{-1} \mathbf{k}_0(n) \mathbf{v}'^{H}_0(n) \mathbf{P}_2(n-1) \tag{48}$$

$$\mathbf{w}'^{H}_0(n) = \mathbf{w}'_2(n-1) + \mathbf{k}_0(n) \xi_0{}^*(n) \tag{49}$$

$$\mathbf{k}_1(n) = \frac{\lambda_1{}^{-1} \mathbf{P}_0(n) \mathbf{v}'_1(n)}{1 + \lambda_1{}^{-1} \mathbf{v}'^{H}_1(n) \mathbf{P}_0(n) \mathbf{v}'_1(n)} \tag{50}$$

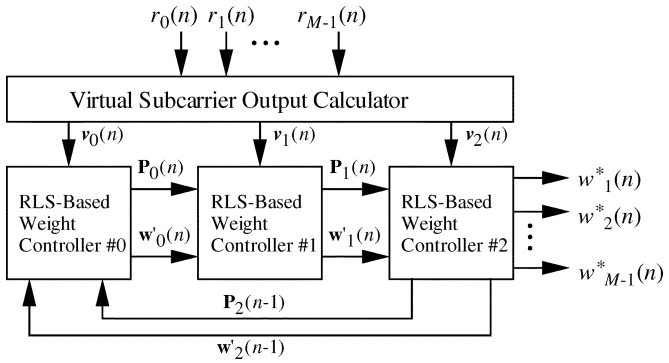

Fig. 5. Multistep RLS-based realization of weight controller.

$$\xi_1(n) = -v_{10}(n) - \mathbf{w}'^{H}_0(n) \mathbf{v}'_1(n) \tag{51}$$

$$\mathbf{P}_1(n) = -\lambda_1{}^{-1} \mathbf{P}_0(n) - \lambda_1{}^{-1} \mathbf{k}_1(n) \mathbf{v}'^{H}_1(n) \mathbf{P}_0(n) \tag{52}$$

$$\mathbf{w}'^{H}_1(n) = \mathbf{w}'_0(n) + \mathbf{k}_1(n) \xi_1{}^*(n) \tag{53}$$

$$\mathbf{k}_2(n) = \frac{\lambda_2{}^{-1} \mathbf{P}_1(n) \mathbf{v}'_2(n)}{1 + \lambda_2{}^{-1} \mathbf{v}'^{H}_2(n) \mathbf{P}_1(n) \mathbf{v}'_2(n)} \tag{54}$$

$$\xi_2(n) = -v_{20}(n) - \mathbf{w}'^{H}_1(n) \mathbf{v}'_2(n) \tag{55}$$

$$\mathbf{P}_2(n) = -\lambda_2{}^{-1} \mathbf{P}_1(n) - \lambda_2{}^{-1} \mathbf{k}_2(n) \mathbf{v}'^{H}_2(n) \mathbf{P}_1(n) \tag{56}$$

$$\mathbf{w}'^{H}_2(n) = \mathbf{w}'_1(n) + \mathbf{k}_2(n) \xi_2{}^*(n) \tag{57}$$

where $\mathbf{k}_j$, $\xi_j(n)$, $\mathbf{P}_j(n)$ ($= \mathbf{\Phi}'^{-1}_j(n)$), and $\mathbf{w}'_j(n)$ (j =0,1,2) are the gain vector ($(M-1) \times 1$), the *a priori* estimation error, the inverse correlation matrix ($(M-1) \times (M-1)$), and the weight vector ($(M-1) \times 1$), respectively. The RLS algorithm given by (46)–(57) contains three updating operations for each instant of time, namely, (46)–(49) calculate $\mathbf{P}_0(n)$ and $\mathbf{w}'_0(n)$ dealing with $\mathbf{P}_2(n-1)$ and $\mathbf{w}'_2(n-1)$ as the old values of the matrix and the vector, respectively, (50)–(53) calculate $\mathbf{P}_1(n)$ and $\mathbf{w}'_1(n)$ dealing with $\mathbf{P}_0(n)$ and $\mathbf{w}'_0(n)$ as the old values of the matrix and the vector, respectively, and (54)–(57) calculate $\mathbf{P}_2(n)$ and $\mathbf{w}'_2(n)$ dealing with $\mathbf{P}_1(n)$ and $\mathbf{w}'_1(n)$ as the old values of the matrix and the vector, respectively. This can be called "a multistep RLS algorithm." Furthermore, as shown in the Appendix, $\mathbf{\Phi}'_2(n)$ and $\mathbf{z}'_2(n)$ satisfy (38) and (39), respectively. Therefore, the optimum weight vector for the cost function of (28) is finally given by

$$\widehat{\mathbf{w}'}(n) = \mathbf{w}'_2(n). \tag{58}$$

Fig. 5 shows the block diagram of the multistep RLS-based realization of the weight controller. Note that the proposed null-steering method uses three different virtual subcarriers to form a beam pattern, so the assumption of (1) is required to make the spatial signature seen by the array be almost the same for the three virtual subcarriers [16].

IV. Numerical Results and Discussions

To demonstrate the performance of the proposed null-steering OFDM adaptive array antenna by computer simulation, the system model for the 1 k-full mode FPU is assumed for the E band with $f_c = 10.35$ GHz [7]. The system generates 856 subcarriers with 1024-point FFT and one midvirtual subcarrier is included ($K_{\text{low}} = 82$, $K_{\text{mid}} = 511$, $K_{\text{high}} = 940$, and

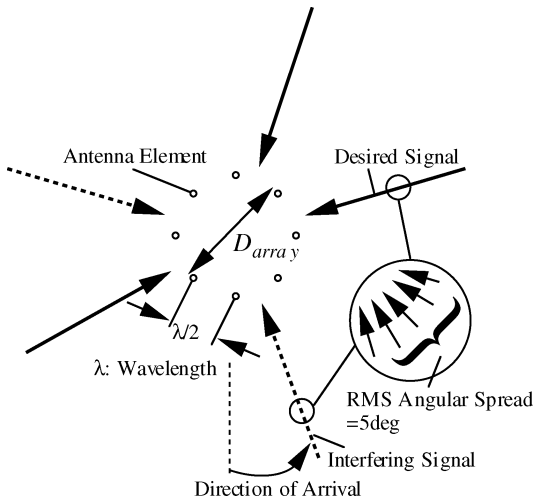

Fig. 6. Incident signal model.

TABLE I
TRANSMISSION-SYSTEM PARAMETERS

Carrier Frequency	10.35 GHz
FFT Size	1024
Number of Subcarriers (K_{sc})	856 (including Pilot Subcarriers)
Subcarrier Separation (Δf_{sc})	19.97 kHz
Oversampling Factor	4
Useful Symbol Length	50.07 μsec (N_U =1024×4 sampls)
Guard Interval Length	6.26 μsec (N_G =128× 4 samples)
Modulation/Detection	QPSK/Coherent Detection
Channel Coding/Decoding	Convolutional Encoding/ Viterbi Decoding (R=1/2, K=7)
Array Configuration	8-element Circular Array with Element Spacing of Half Wavelength
Number of Virtual Subcarriers Used	3 K_{low}=82, K_{mid}=511, K_{high}=940

$K_{sc} = 1024$). In addition, the useful symbol length is 50.07 μs, which corresponds to 1024 samples, whereas the guard interval length is 6.26 μs (128 samples). Furthermore, for a modulation and detection format, coherent quadrature phase-shift keying (QPSK) is assumed and, for a channel-coding format, a half-rate ($R = 1/2$) convolutional code with constraint length of 7 ($K = 7$) is assumed and the oversampling factor of 4 is employed.

Fig. 6 shows the incident signal model. For an array configuration, an eight-element circular antenna array with element spacing of half wavelength is assumed. Each signal is assumed to arrive in a cluster and the cluster is composed of five components with root-mean-square (rms) angular spread of 5° and the difference of arrival time among the components in the cluster is negligibly small. Therefore, the resultant envelope is almost Rayleigh distributed and it means that $\alpha_{Dh,m}$ and $\alpha_{Il,m}$ can be dealt as mutually independent complex-valued Gaussian random variables with an average of zero. Here, defining their powers as $\sigma^2_{Dh,0} = \cdots \sigma^2_{Dh,7} = \sigma^2_{Dh}$ and $\sigma^2_{Il,0} = \cdots \sigma^2_{Il,7} = \sigma^2_{Il}$, respectively. They are assumed to be identical, namely, $\sigma^2_{D0} = \sigma^2_{D1} = \cdots, \sigma^2_{DL_D} = \sigma^2_D$, and $\sigma^2_{I0} = \sigma^2_{I1} = \cdots, \sigma^2_{IL_I} = \sigma^2_I$. Furthermore, the average power ratio of desired signal to interfering signal (Average $D/I = \sigma^2_D/\sigma^2_I$) is set to 0 dB. The DoA for the desired signal is randomly chosen from the region of (0°, 360°] and the interfering signal is also randomly chosen from the angular region, where the two kinds of signals are not overlapped. For the null-steering array antenna, the algorithm requires no special pilot signal, so it can be employed repeatedly in many OFDM symbol periods. However, in Figs. 7–11, it is employed only in one OFDM symbol period. Table I summarizes the transmission system parameters. Note that (1) is satisfied for the parameters in Table I.

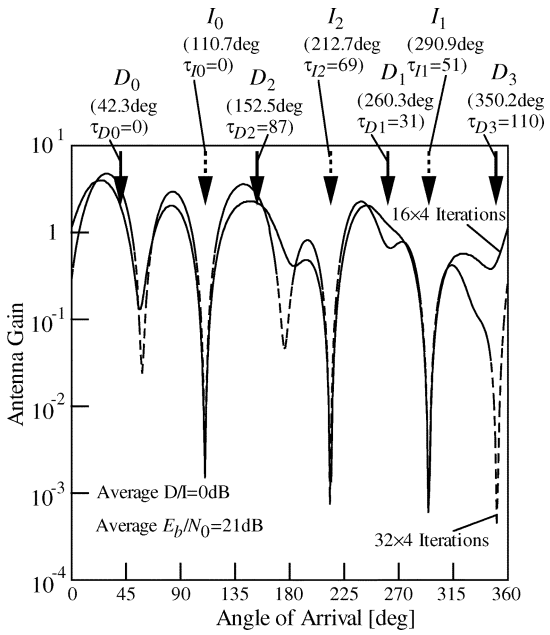

Fig. 7. Array antenna pattern.

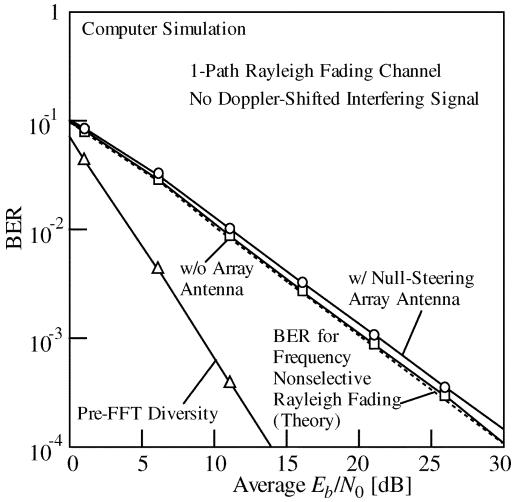

Fig. 8. BER for the case of one desired signal and no interfering signal.

Fig. 7 shows an example of the antenna pattern for the case where there are four desired components and three interfering components. The time delay for the fourth desired components (D_3) is 110 samples, so nulls are steered toward not only the interfering signals (I_0, I_1, and I_2), but also D_3 when setting $W_o = 32$ ($T_W = 96$), whereas nulls are steered only toward I_0, I_1 and I_2 when setting $W_o = 16$ ($T_W = 112$). There is no large difference in the depth of null for $W_o = 32$ and $W_o = 16$; therefore, in the following, W_o is set to 16. In addition to it,

TABLE II
$\{\beta_d\}$

d	β_d
d_{free} (=10)	36
$d_{free}+1$	0
$d_{free}+2$	211
$d_{free}+3$	0
$d_{free}+4$	1404

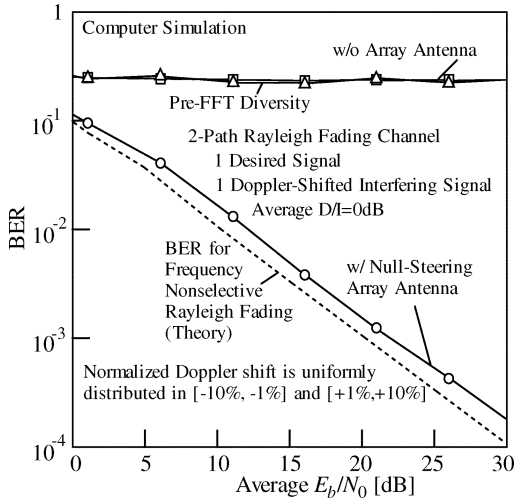

Fig. 9. BER for the case of one desired signal and one interfering signal.

the arrival time of interfering signal is assumed to be uniformly distributed within the guard interval (0 samples, 127 samples) and that of desired signal is assumed to be uniformly distributed within (0 samples, 111 samples).

Fig. 8 shows the BER of the null-steering array antenna versus the average E_b/N_0 for the case of one desired signal and no interfering signal. In this figure, for comparison, the BERs without array antenna (namely, an omnidirectional antenna) and for the pre-FFT space diversity antenna [10] are shown. The pre-FFT space diversity antenna is optimal in the sense that it can maximize the signal-to-noise power ratio if there is no interference. The computational complexity of the pre-FFT space diversity antenna is proportional to M^3, namely, $O(M^3)$, because it calculates the array weight vector associated with the largest eigenvalue for the autocorrelation matrix of the received signal [17]. On the other hand, the computational complexity of the null-steering array antenna is $O(M^2)$ because its control is based on the RLS algorithm [17]. Therefore, the null-steering array antenna is advantageous in terms of computational complexity. The BER without array antenna, which is equivalent to that for frequency-nonselective Rayleigh fading, is theoretically given by

$$\mathrm{BER}_{fn} = \sum_{d=d_{\mathrm{free}}}^{+\infty} \beta_d P(d) \tag{59}$$

$$P(d) = \int_0^{+\infty} \sum_{u=0}^{d-1} \binom{d-1+u}{u} (1-p(\gamma_b))^u p(\gamma_b) d\gamma_b \tag{60}$$

$$p(\gamma_b) = \frac{1}{\Gamma_b} e^{-\gamma_b/\Gamma_b} \tag{61}$$

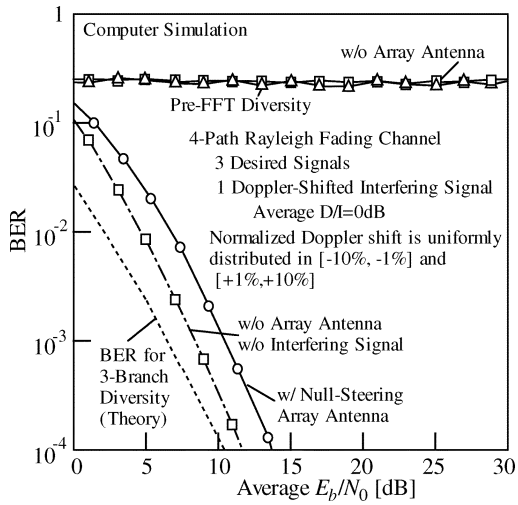

Fig. 10. BER for the case of three desired signals and one interfering signal.

where d_{free} is the free distance of the convolutional code, β_d is the weight coefficient calculated from the transfer function of the convolutional code, γ_b is the instantaneous ratio of energy-per-bit to power spectral density of noise, and $p(\gamma_b)$ is the probability density function (pdf) of γ_b [18]. In the numerical calculation, the summation is upper-limited by $d = d_{\mathrm{free}} + 4$. Table II shows the values of the weights [19]. The pre-FFT space diversity antenna has the eighth-order space diversity gain, so the BER performance is excellent. On the other hand, the null-steering array antenna has no space diversity gain, so the BER performance is close to that without array antenna. In this case, the null-steering array antenna should act as an omnidirectional antenna, but the antenna pattern is controlled by (23), namely, the noise at the virtual subcarrier output. Therefore, as compared with the case without array antenna, the null-steering array antenna has a small degradation of around 0.5 dB at the BER of 10^{-3}.

Fig. 9 shows the BER versus the average E_b/N_0 for the case of one desired signal and one interfering signal. Here, the Doppler shift of the interfering signal is uniformly distributed in $[-10\%, -1\%]$ and $[+1\%, +10\%]$. Without an array antenna, the BER performance is poor and flat. Furthermore, even with the pre-FFT space diversity antenna, it cannot distinguish the desired components from the interfering ones, so the BER performance also is poor and flat. On the other hand, the null-steering array antenna suppresses the interfering signal and tries to keep the BER performance close to that of an omnidirectional antenna without interference, so a much better BER performance is obtained. As compared with the theoretical BER, the null-steering array antenna has a degradation of around 1 dB at the BER of 10^{-3}. This is because a lower antenna gain is formed for the desired signal when the angle difference between the desired and interfering signals is small.

Fig. 10 shows the BER versus the average E_b/N_0 for the case of three desired signals and one interfering signal. The omnidirectional antenna and the pre-FFT space diversity antenna do not work well at all. On the other hand, the null-steering array antenna has the third-order path diversity gain and the BER performance is close to that of an omnidirectional antenna without

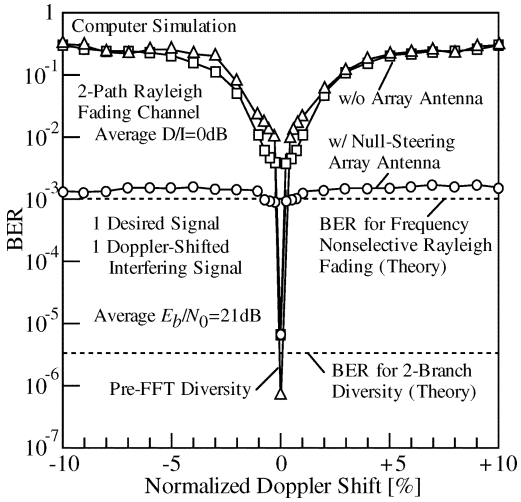

Fig. 11. BER versus Doppler shift.

interference. The BER of an l_a-branch diversity is theoretically given by [18]

$$\mathrm{BER}_{l_a b} = \left[\frac{1}{2}(1-\rho)\right]^{l_a} \sum_{x=0}^{l_a-1} \binom{1+x}{x} \left[\frac{1}{2}(1+\rho)\right]^{x} \quad (62)$$

$$\rho = \sqrt{\frac{\Gamma_b}{1+\Gamma_b}}. \quad (63)$$

Fig. 11 shows the BER versus the Doppler shift normalized by the subcarrier separation for the case of one desired signal and one interfering signal. When the magnitude of the normalized Doppler shift is around 0%, the interfering signal acts as another desired signal, so the null-steering array antenna has the second-order path diversity gain. The BER for $\Delta f'_{I1} = 0$ is given by (62) with $l_a = 2$. On the other hand, when the magnitude of the normalized Doppler shift exceeds 1%, without array antenna, the interfering signal gives an intolerable degradation to the BER performance; however, the null-steering array antenna can make the BER around the level attainable for the case without interference. The null-steering array antenna can work well for the wide range of the normalized Doppler shift and when the magnitude of the normalized Doppler shift exceeds 1%, the BER performance is flat and insensitive to the value of the Doppler shift. The pre-FFT space diversity antenna can give an excellent BER only for the small Doppler shift of around 0% with the second-order path diversity gain as well as the eighth-order path diversity gain. However, when the magnitude of the normalized Doppler shift exceeds 1%, there is no large difference in BER performance between the omnidirectional antenna and the re-FFT space diversity antenna.

V. Conclusion

This paper has proposed a simple null-steering method to suppress Doppler-shifted signals for a pre-FFT type OFDM adaptive array antenna. The null-steering array antenna does not try to effectively catch desired signals, but it can well suppress Doppler-shifted interfering signals by forcing virtual subcarrier outputs to be zero. A multistep RLS has been discussed to control the array weights. The null-steering array antenna gives no space diversity gain, but even with interfering signals with small Doppler shifts, it tries to keep the BER performance close to that of an omnidirectional antenna without interference.

Appendix

Multistep RLS Algorithm

Substituting (40) and (41) into (42) leads to

$$\mathbf{\Phi}'_2(n) = \lambda_0\lambda_1\lambda_2\mathbf{\Phi}'_2(n-1) + \lambda_1\lambda_2\mathbf{v}'_0(n)\mathbf{v}'^{H}_0(n) + \lambda_2\mathbf{v}'_1(n)\mathbf{v}'^{H}_1(n) + \mathbf{v}'_2(n)\mathbf{v}'^{H}_2(n). \quad (64)$$

Similarly, substituting (43) and (44) into (45) leads to

$$\mathbf{z}'_2(n) = \lambda_0\lambda_1\lambda_2\mathbf{z}'_2(n-1) - \lambda_1\lambda_2\mathbf{v}'_0(n)v'^{*}_{00}(n) - \lambda_2\mathbf{v}'_1(n)v'^{*}_{10}(n) - \mathbf{v}'_2(n)v'^{*}_{20}(n). \quad (65)$$

Setting $\lambda_0 = \lambda$, $\lambda_1 = 1.0$ and $\lambda_2 = 1.0$ in (64) and (65), they becomes equivalent to (38) and (39), respectively.

Acknowledgment

The authors would like to thank the anonymous reviewers for their helpful comments.

References

[1] "Digital broadcasting systems for television, sound and data services; framing structure, channel coding and modulation for digital terrestrial television," Eur. Telecommun. Standards Inst. (ETSI), ETSI 300 744, 1996.

[2] *Data Coding and Transmission Specification for Digital Broadcasting*, ARIB Standard B24, Jun. 2000.

[3] *Wireless Medium Access Control (MAC) and Physical Layer (PHY) Specifications: High-Speed Physical Layer Extension in the 5 GHz Band*, IEEE Standard 802.11a, 1999.

[4] "Broadband radio access networks (BRAN); HIPERLAN Type2; Physical (PHY) layer," ETSI BRAN, ETSI TR 101 475, 2000.

[5] *Lower Power Data Communication Systems Broadband Mobile Access Communication System (CSMA)*, ARIB Standard T70, Dec. 2000.

[6] *Lower Power Data Communication Systems Broadband Mobile Access Communication System (HiSWANa)*, ARIB Standard T70, Dec. 2000.

[7] *Portable OFDM Digital Transmission System for Television Program Contribution*, ARIB Standard B33, Mar. 2002.

[8] R. A. Monzingo and T. W. Miller, *Introduction to Adaptive Arrays*. New York: Wiley, 1980.

[9] Y. Li and N. R. Sollenberger, "Adaptive antenna arrays for OFDM systems with cochannel interference," *IEEE Trans. Commun.*, vol. 47, no. 2, pp. 217–229, Feb. 1999.

[10] M. Okada and S. Komaki, "Pre-FFT combining space diversity assisted COFDM," *IEEE Trans.Veh. Technol.*, vol. 50, no. 2, pp. 487–496, Mar. 2001.

[11] S. Hara, A. Nishikawa, and Y. Hara, "A novel OFDM adaptive antenna array for delayed signal and Doppler-shifted signal suppression," in *Proc. IEEE ICC'01*, Helsinki, Finland, Jun. 2001, pp. 2302–2306.

[12] S. Hara, S. Hane, and Y. Hara, "Adaptive antenna array for reliable OFDM transmission," in *Proc. 6th Int. OFDM Workshop*, Hamburg, Germany, Sep. 2001, pp. 1.1–1.4.

[13] H. Liu and U. Tureli, "A high-efficient carrier estimator for OFDM communications," *IEEE Commun. Lett.*, vol. 2, pp. 104–106, Apr. 1998.

[14] C. Y. Li and S. Roy, "Subspace-based blind channel estimation for OFDM by exploiting virtual carriers," *IEEE Trans. Wireless Commun.*, vol. 2, no. 1, pp. 141–150, Jan. 2003.

[15] S. Barbarossa, M. Pompili, and G. B. Giannakis, "Channel-independent synchronization of orthogonal frequency division multiple access systems," *IEEE J. Sel. Areas Commun.*, vol. 20, no. 2, pp. 474–486, Feb. 2002.

[16] M. A. Lagunas, A. I. P. Neira, M. G. Amin, and J. Vidal, "Spatial processing for frequency diversity schemes," *IEEE Trans. Signal Process.*, vol. 48, no. 2, pp. 353–362, Feb. 2000.

[17] S. Haykin, *Adaptive Filter Theory*, 3rd ed. Englewood Cliffs, NJ: Prentice-Hall, 1996.

[18] J. G. Proakis, *Digital Communications*, 4th ed. New York: McGraw-Hill, 2001.
[19] J. Conan, "The weight spectra of some short low-rate convolutional codes," *IEEE Trans. Commun.*, vol. 32, no. 9, pp. 1050–1053, Sep. 1984.

Shinsuke Hara (S'88–M'90) received the B.Eng., M.Eng., and Ph.D. degrees in communications engineering from Osaka University, Osaka, Japan, in 1985, 1987, and 1990, respectively.

From April 1990 to March 1996, he was an Assistant Professor in the Department of Communication Engineering, Osaka University. Since April 1996, he has been with the Department of Electronic, Information System and Energy Engineering, Graduate School of Engineering, Osaka University, where he currently is an Associate Professor. Also, from April 1995 to March 1996, he was a Visiting Scientist with the Telecommunications and Traffic Control Systems Group, Delft University of Technology, Delft, The Netherlands. His research interests include mobile and indoor wireless communications systems and digital signal processing.

Shuichi Hane received the B.Eng. degree in communications engineering and the M.Eng. degree in electronic, information system, and energy engineering from Osaka University, Osaka, Japan, in 2001 and 2003, respectively.

Since April 2003, he has been with Tokyo Electric Power Company, Inc., Tokyo, Japan. His research interests include the design and performance analysis of communication systems.

Yoshitaka Hara (M'02) received the B.E., M.E., and Dr.Eng. degrees from the University of Tokyo, Tokyo, Japan, in 1993, 1995, and 2003, respectively.

In 1996, he joined Mitsubishi Electric Corporation, Kanagawa, Japan. From 1999 to 2001, he also was a Senior Research Engineer with YRP Mobile Telecommunications Key Technology Research Laboratories Co. Ltd., Kanagawa, Japan. Since 2003, he has been with the Mitsubishi Electric Information Technology Centre Europe B.V. (ITE), Rennes, France. His research interests include CDMA systems and adaptive antenna arrays.